Proceedings World Geothermal Congress 2005
Antalya, Turkey, 24-29 April 2005

Thermal Modeling of the Hot Dry Rock Geothermal Resource Beneath GEL99 in the Cooper Basin, South Australia

Graeme R. Beardsmore

School of Geosciences, Monash University, Victoria, 3800, Australia

gbeards@mail.earth.monash.edu.au

Keywords; HDR, Australia, heat flow

ABSTRACT

Radiogenic granites beneath the Cooper Basin are purported to be the most prospective hot dry rock resource in the world, but the remote location means that any economic development of the resource must factor in a significant cost of connecting to the national electricity grid. This cost cannot be easily reduced. The other major cost of development is drilling, so it is imperative to keep this cost to a minimum. As the energy potential of the rocks is directly proportional to their temperature, it is vital to target drilling at locations likely to yield the highest temperatures at the shallowest depths.

The South Australian government has granted three Geothermal Exploration Leases for commercial ventures to explore in the Cooper Basin. GEL99 is one of those leases and is currently operated by Scopenergy Limited. A series of one-dimensional conductive heat flow models were developed from thermal conductivity profiles and bottom hole temperature data extracted from numerous petroleum exploration and appraisal wells in the GEL99 area. These heat flow estimates were then extrapolated vertically into the underlying crystalline basement to predict the temperature versus depth distribution at specific points in the region.

The conductive heat flow at the top of the Warburton Basin sequence was found to be about 103±8 mWm^2 beneath most of GEL99. The 220°C isotherm lies at a mean depth of around 4200–4300 m beneath most of the wells studied. Heat flow appears to be closely related to the nature of the basement rocks.

1. INTRODUCTION

1.1 Hot dry rock exploration in Australia

"Hot dry rock" geothermal developments aim to superheat water by pumping it down to and through crystalline rocks with an ambient temperature of at least 220°C. Hot water or steam is extracted via a second borehole and used to drive conventional electricity generator turbines, either directly, or via secondary steam generation using a heat exchanger.

Radiogenic plutons beneath the Cooper Basin in South Australia and Queensland (Figure 1) are purported to be the most prospective hot dry rock resource in the world (e.g. Swenson *et al.*, 2000). The South Australian Government has granted three Geothermal Exploration Leases (GELs) in the Cooper Basin for the purpose of hot dry rock geothermal energy investigations (Figure 1). Two companies have been awarded the rights to the permits. Geodynamics Limited controls GEL97 and GEL98, while Scopenergy Limited currently operates GEL99.

The remote location impacts strongly on the economics of any proposed commercial energy development. Total cost projections for developing the resource must factor in a significant cost for connection to the national electricity grid. This cost cannot be easily reduced. Drilling represents the other major cost of development, so it is imperative to keep this cost to a minimum. The commercial value of the resource lies in the energy potential of the rocks, which is directly proportional to their temperature. The economic viability of the project is therefore maximized if drilling is targeted towards those locations where the critical 220°C isotherm is at the shallowest depth.

The aim of this project was to estimate the distribution of temperature within crystalline rocks beneath GEL99, using bottom hole temperatures and lithological information derived from petroleum industry boreholes in the vicinity of the permit. The results are to be used in subsequent studies to assess the economic viability of the resource.

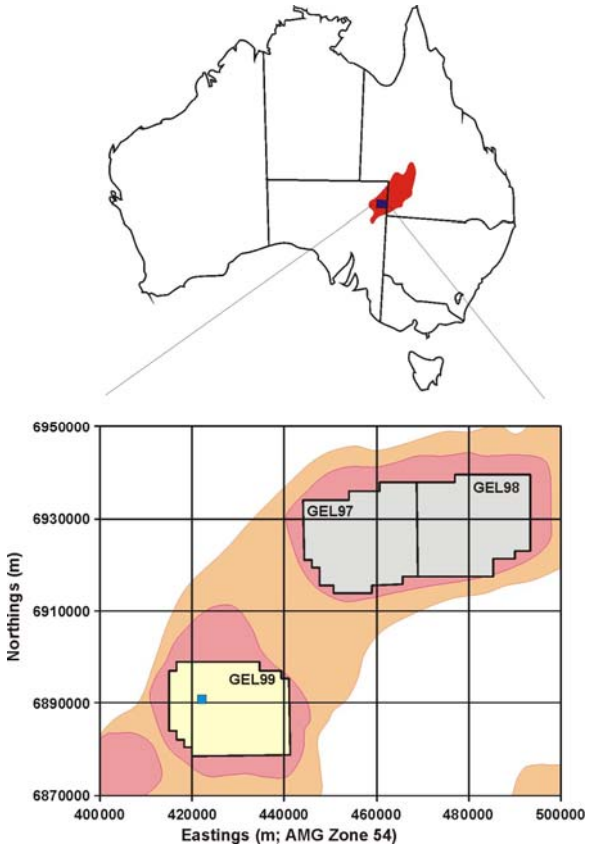

Figure 1. Location of Geothermal Exploration Permits within the Cooper Basin (red area on top map). Pink regions show the extent of granitic bodies as interpreted from regional gravity data (light = deeper, dark = shallower); Data from Boucher (2002). Blue square = Moomba township.

1.2 The geology beneath GEL99

GEL99 is underlain by four distinct basin sequences atop a basement of Proterozoic meta-sediments (Boucher, 2002;

Figure 2). The Proterozoic sequence played no direct role in this project and will not be discussed further.

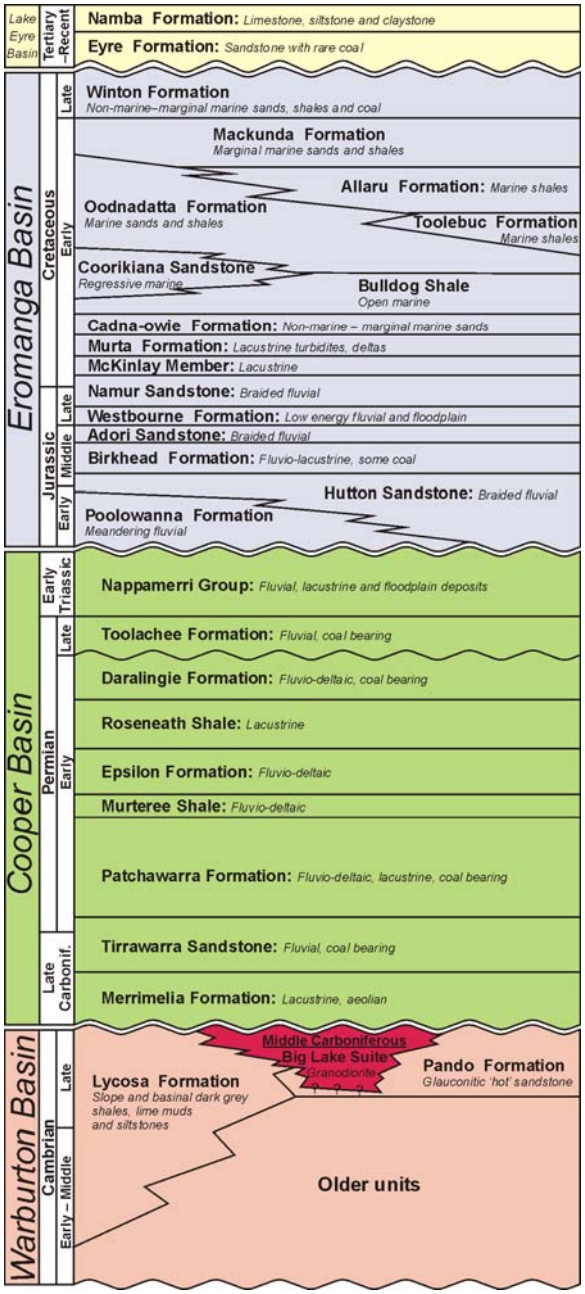

Figure 2. Simplified stratigraphy beneath GEL99. Note that only those units intercepted by the study wells are shown.

The Cambrian–Ordovician aged Warburton Basin sequence is the "basement" for this project. It is primarily composed of volcanics and shallow-marine/delta formations, but also hosts the Carboniferous-aged granodiorite intrusive known as the Big Lake Suite (Boucher, 2002). The Big Lake Suite is thought to be the primary source of crustal heat generation in the region. Two other formations of interest to this project are the Pando Formation—a bioturbated, glauconitic, radiogenic sandstone—and the Lycosa Formation—an interbedded siltstone and limey mudstone.

The Late Carboniferous–Early Triassic Cooper Basin overlies the Warburton unconformably, and is one of the most mature petroleum exploration provinces in Australia. The sediments within the basin have been comprehensively investigated and described in the literature. They include extensive Permian coal sequences that create an efficient thermal blanket above the "hot" intrusive body. The Cooper Basin sequence varies between 700–1000 m thick in most of the study wells.

The Early Jurassic–Late Cretaceous Eromanga Basin lies unconformably on top of the Cooper Basin. The deeper formations are predominantly fluvial sandstones, but the younger formations grade into marginal and open marine sediments. The youngest unit is the coal-bearing Winton Formation. The Eromanga Basin sequence is between 1800–2000 m thick in most of the study wells.

The Tertiary–Recent Lake Eyre Basin overlies the entire region. It is uniformly between 250–300 m thick and composed primarily of fluvial and lacustrine deposits.

1.3 Previous thermal studies

Middleton (1979) and Gallagher (1987a) published thermal conductivity and heat generation values for a number of Cooper and Eromanga Basin formations. Gallagher (1987b) used these values to estimate heat flow in a number of wells geographically spread over the Cooper Basin.

More recently, Deighton and Hill (1998) summarized and extended on earlier paleo-heat flow studies to model the full thermal history of the Cooper Basin sequence and its implications for petroleum generation. They drew on the results of apatite fission track and vitrinite reflectance studies, combined with present day bottom hole temperature estimates. Their study encompassed the whole of the South Australian portion of the Cooper Basin, and only superficially covered the GEL99 area.

The Department of Primary Industries and Resources, South Australia (PIRSA) has compiled a database of petroleum exploration borehole information. The database, called the "Petroleum Exploration and Production System—South Australia" ("PEPS-SA"), contains a wealth of information from close to 2000 petroleum exploration, development and appraisal wells across the state of South Australia. Information includes locations, elevations, formation names and depths, down-hole temperature measurements, formation fluid test results, geochemical paleotemperature indicators and hydrocarbon occurrences. PEPS-SA was the major data source for this project.

2. METHODOLOGY

The first stage of the project was to calculate reliable estimates of vertical conductive heat flow at a number of well locations in the region of GEL99. The next stage was to downward continue these estimates into the crystalline basement to predict the temperature distribution to a depth of five kilometers.

Conductive heat flow is the product of thermal gradient and thermal conductivity, modified by internal heat generation. In order to calculate vertical heat flow estimates within GEL99, it was, therefore, necessary to identify those wells from which reliable temperature data, thermal conductivity profiles and heat generation estimates could be extracted. The following sections describe this process in detail.

2.1 Temperature data

Two temperature values at different depths are required to define a thermal gradient. Average surface temperature is generally used for the upper constraint. The Australian Bureau of Meteorology lists the average annual maximum and minimum temperatures at the township of Moomba as 29.0°C and 14.9°C, respectively (http://www.bom.gov.au/climate/averages/tables/cw_017096.shtml). Taking into account the albedo of the surface layer of the Earth (e.g. Beardsmore and Cull, 2001, p78), the average temperature of the surface layer at Moomba is probably close to 25°C. This value was adopted across the entire study region.

For deeper temperatures, I extracted all temperature data from PEPS-SA for the region in Australian Map Grid (AMG) Zone 54 (Australian Geodetic Datum, 1966) bounded by 410,000–450,000 E and 6,870,000–6,910,000 N. This area coincides with the location of a number of major gas fields, so there were data from several hundred wells. I only wished to use data of high reliability, so applied a sampling filter. Bottom hole temperature (BHT) data were accepted as reliable only if they conformed to the following selection criteria:

1) Estimated BHTs (as recorded in PEPS-SA) were calculated by Horner correction of a minimum of three raw BHT values recorded at different times and within 50 vertical meters of each other.

2) Estimated BHTs were consistent with Cement Bond Log (CBL) temperatures recorded a significant time after mud circulation at a similar depth.

The filter reduced the sample to a set of 11 wells, as shown on Figure 3. In addition, the wells Moomba North 1 and 2 were also examined because of reported high gradients in Moomba North 1.

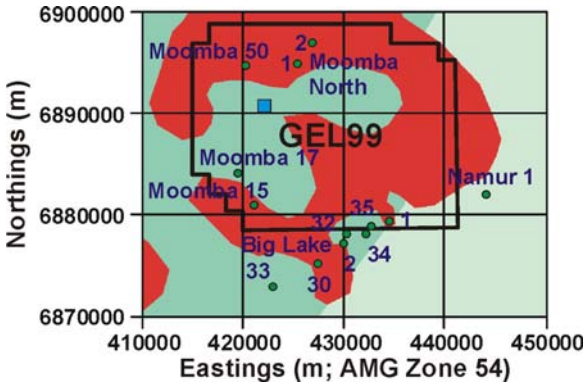

Figure 3. Names and locations of study wells, superimposed on Cooper Basin subcrop map. Blue square = Moomba township. Subcrop: red = Big Lake Suite; pale blue = Lycosa Formation; dark blue = Pando Formation (modified after Boucher, 2002).

PEPS-SA also records drill stem test (DST) and cased hole test (CHT) temperatures, which are often cited as being very reliable (e.g. Beardsmore and Cull). Anecdotally, however, many data recorded as DST values are, in fact, from other, less reliable, types of tests. The DST and CHT values recorded for the sample wells were noted, but assumed to be of lower reliability than other temperature data.

2.2 Thermal conductivity models

A table of formation tops was extracted from the PEPS-SA database for each of the study wells. The average vertical thermal conductivity for each well was determined from the harmonic mean of the conductivities of the penetrated formations. The thermal conductivity of each formation was assigned using the following methods.

2.2.1 Conductivity as measured by Gallagher (1987a)

Gallagher (1987a) published thermal conductivity measurements for a number of Cooper Basin formations, including the Big Lake Suite. Gallagher's measurements were adopted as the thermal conductivities of those formations with relatively homogenous lithology. However, where his measurements were thought to represent only a portion of the sampled formation, the bulk conductivity of the formation was derived by alternative means.

2.2.2 Conductivity calculated from lithological proportions as supplied by PIRSA

The thermal conductivity of a rock is primarily a function of grain matrix mineralogy. The average conductivity of a formation can be estimated if the relative proportions of each rock type, and the thermal conductivities of those rock types, are known for the formation. PIRSA supplied a spreadsheet listing the proportions of sandstone, siltstone, shale and coal in five Cooper Basin formations (Nappamerri Group, Toolachee Formation, Daralingie Formation, Epsilon Formation, Patchawarra Formation). The lithological proportions had been extracted from detailed analyses of electric well logs and cuttings. By assuming that the lithologies formed roughly horizontal layers, the average thermal conductivity of each formation in each well was determined from the harmonic mean conductivity of its constituent lithologies.

2.2.3 Conductivity calculated from lithological proportions as derived from cuttings logs in well completions reports.

For the remaining formations, lithological proportions were estimated from drill cutting descriptions in well completion reports. A number of reports were examined from geographically scattered wells. Average compositions were calculated for each formation, and thermal conductivity determined from the harmonic mean of the constituents.

2.2.4 Pore fluid correction

Thermal conductivity is also a function of pore fluid composition. Water is generally assumed to inhabit all available pore space, but gas is present in a number of units within the Cooper Basin. Gas is a thermal insulator compared to water, and serves to reduce the thermal conductivity of a formation by an average of about 25% where present. This effect was taken into account for those formations known (from PEPS-SA) to contain gas, and was found to reduce the calculated heat flow by as much as 5 mW/m^2 in some wells.

2.2.5 Uncertainty in average conductivity

The standard deviation (σ) of the average thermal conductivity was calculated as $\sqrt{\Sigma(\sigma_i^2)}$, where σ_i was the standard deviation of the conductivity estimate of each individual layer.

2.3 Heat generation

Sediments commonly generate little heat, on the order of 0–2 $\mu W/m^3$ (e.g. McKenna and Sharp, 1998; Keen and Lewis, 1982). In general, shale and claystone generate heat at a

greater rate than sandstone and limestone. Gallagher (1987b) provided data that suggest that Cooper Basin sediments generate heat at an average rate of between 0.9–1.5 $\mu W/m^3$. Over a three-kilometer sedimentary section, it is likely, therefore, that the addition of heat from sediments is less than 4 mW/m^2. In the absence of advective heat transfer within the section, the heat flow at the base of a well should vary by less than 2 mW/m^2 from the average heat flow within the well. Given the magnitude of heat flow estimates calculated in this study, heat generation within the sediment column was considered negligible and ignored.

Heat generation within the Big Lake Suite, however, is significant, and is believed to be the major source of the elevated heat flow observed at the surface. Values from 7.5–10.3 $\mu W/m^3$ have been reported (Middleton, 1979), and 10 $\mu W.m^3$ was used in the models to yield conservative estimates of basement temperature. This value causes the modeled heat flow to decrease by 10 mW/m^2 for each kilometer of penetration into the basement granite.

2.4 1D models

One-dimensional thermal models were constructed in stages. All calculations were performed using spreadsheet software. Each well was processed independently according to the following procedure.

The first step was to extract the stratigraphic data for the well from PEPS-SA. Information included formation name, top depth and thickness. Each formation was assigned an initial thermal conductivity according to the procedure detailed in Section 2.2. The temperature at the surface was assumed to be 25°C, and the temperature at the base of the well was estimated from the temperature data in PEPS-SA, as described in Section 2.1.

The thermal conductivity, λ, and thickness, Δz, of each unit was then converted into a "thermal resistance" for the unit. Thermal resistance, R, is the physical thickness divided by the thermal conductivity:

$$R = \Delta z / \lambda \quad (1)$$

In a steady state conductive heat flow regime, temperature increases linearly with thermal resistance. The next step, therefore, was to use this fact to establish an approximate temperature profile through the sequence. A temperature correction was then applied to the thermal conductivity of each formation, following the method of Sekiguchi (1984):

$$\lambda = (T_0 T_m/(T_m-T_0))(\lambda_0-\lambda_m)((1/T)-(1/T_m))+\lambda_m \quad (2)$$

where λ_m = 1.05 W/mK; λ_0 = initial thermal conductivity (W/mK) of the formation; T_0 = temperature (K) at which λ_0 was measured (assumed 298 K); T_m = 1473 K.

Correcting the thermal conductivity profile of the sequence had the effect of altering the thermal resistance of each formation. The calculated temperature profile also changed, suggesting that the temperature correction could be further refined. Additional temperature corrections were found to have little effect on the results, however, and were ignored.

The heat flow estimate, Q (mW/m^2), for the well was:

$$Q = \Delta T / \Sigma R \quad (3)$$

Where ΔT = total temperature drop across the well = bottom hole temperature – surface temperature; ΣR = total thermal resistance of the sequence = the sum of the thermal resistances of all the individual formations.

The relative uncertainty in the heat flow estimate was equivalent to the uncertainty in ΣR. This, in turn, was related to the uncertainty in the thermal conductivity of the individual formations. The relative uncertainty in ΣR, $\Delta\Sigma R$, was:

$$\Delta\Sigma R = \sqrt{\Sigma[R_i \times (\Delta\lambda_i/\lambda_i)]^2} \quad (4)$$

where R_i, $\Delta\lambda_i$ and λ_i are, respectively, the thermal resistance, standard deviation of thermal conductivity, and mean thermal conductivity of each successive layer.

Once the vertical conductive heat flow was known for a well, the value was extrapolated into the basement to predict the thermal conditions below the bottom of the hole. The basement was assumed to be granodiorite in all instances. Temperatures were calculated at 100 m intervals down to 5 km, assuming a thermal conductivity of 3.2±0.4 W/mK (Gallagher, 1987a) and heat generation of 10 $\mu W/m^3$. A temperature correction was not required because the thermal conductivity of granite varies little with temperature (Touloukian *et al*., 1970).

3. RESULTS

The results for each study well are presented as a modeled temperature profile, with all reported temperature data and major stratigraphic boundaries shown on the figure. The profiles provide a direct comparison between the model results and the reported data, and allow an objective assessment of the reliability of each model.

On each figure, green circles represent DST and CHT data; blue circles are corrected BHT values; red circles are CBL temperatures; the black line shows the modeled thermal profile within the well; dashed black line (on some plots) is the straight-line gradient between the surface and the CBL temperature; the purple line is the extrapolated thermal profile below the well; horizontal brown lines show boundaries between major basin sequences; vertical red line marks the 220°C isotherm. Error bars on the extrapolated section of the profile are ±1σ, taking into account the uncertainty in the conductivity of the basement and the uncertainty in the heat flow estimate.

Results are summarized in Table 1. A discussion of the results is included in the next section.

Table 1. Results of 1D models. Q_b = heat flow at top of basement (mW/m^2); T_{4km} = temperature at 4 km (°C); T_{5km} = temperature at 5 km (°C); Z_{220} = depth range of 220°C isotherm (mKB; 5km maximum); BL = Big Lake; M = Moomba; MN = Moomba North; N = Namur. Uncertainties are ±1σ.

Well	Q_b	T_{4km}	T_{5km}	Z_{220}
BL1	102±8	219±6	246±11	3875–4323
BL2	102±8	212±16	239±22	3770–>
BL30	87±7	189±5	212±9	>5000
BL32	105±8	215±7	243±13	3943–4514
BL33	89±7	197±5	220±9	4647–>
BL34	101±8	215±6	242±11	3976–4484
BL35	103±8	218±6	246±11	3877–4322
M15	95±9	206±17	231±22	3895–>
M17	102±6	211±15	238±20	3835–>
M50	103±8	222±6	249±12	3787–4196

MN1	103±8	218±6	246±11	3909–4336
MN2	106±8	215±6	243±12	3964–4483
N1	113±10	204±10	233±16	4159–>

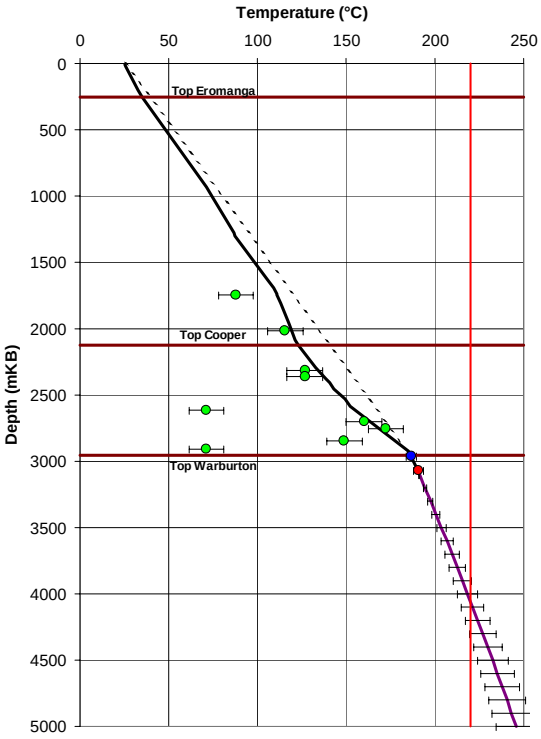

Figure 4. Temperature data and modeled profile for Big Lake 1.

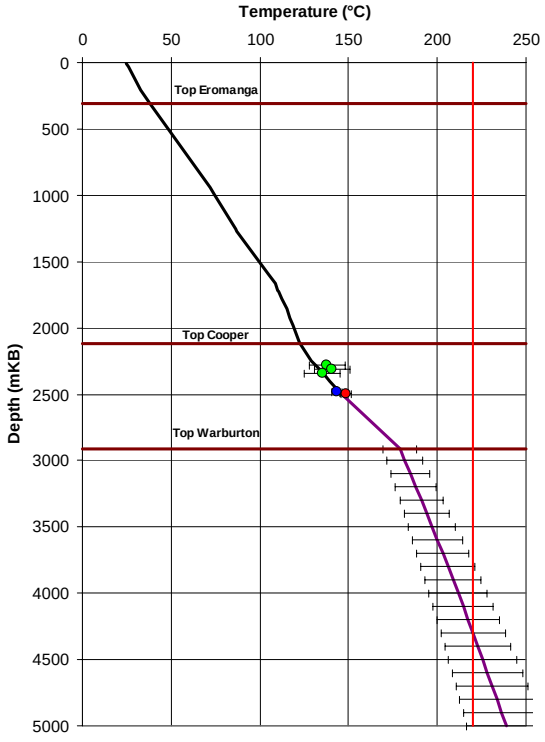

Figure 5. Temperature data and modeled profile for Big Lake 2.

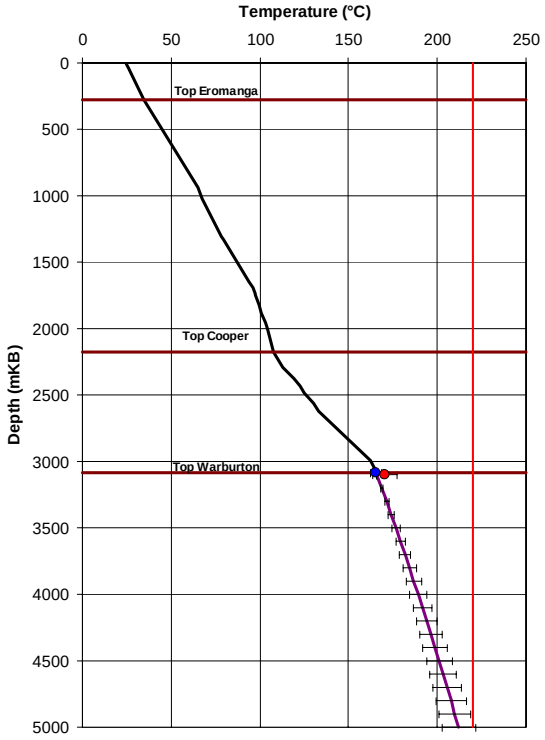

Figure 6. Temperature data and modeled profile for Big Lake 30.

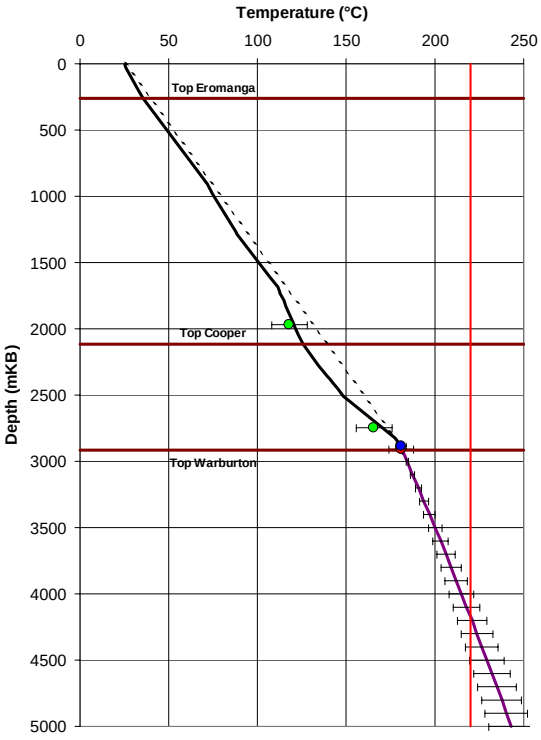

Figure 7. Temperature data and modeled profile for Big Lake 32.

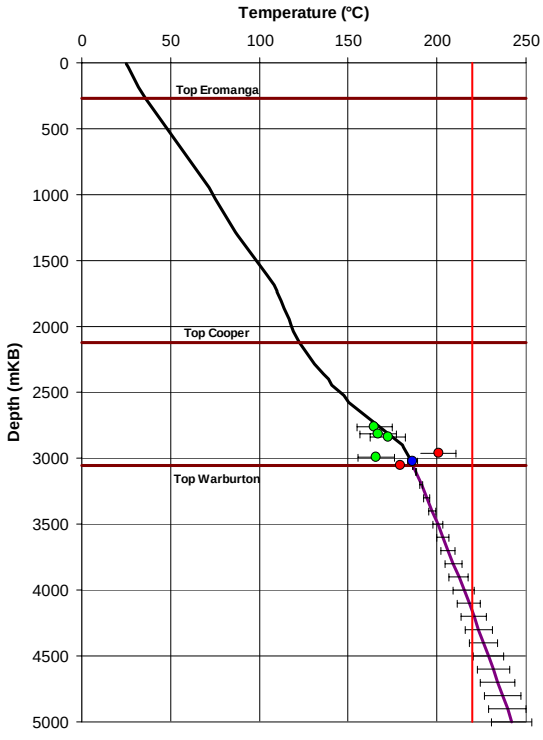

Figure 9. Temperature data and modeled profile for Big Lake 34.

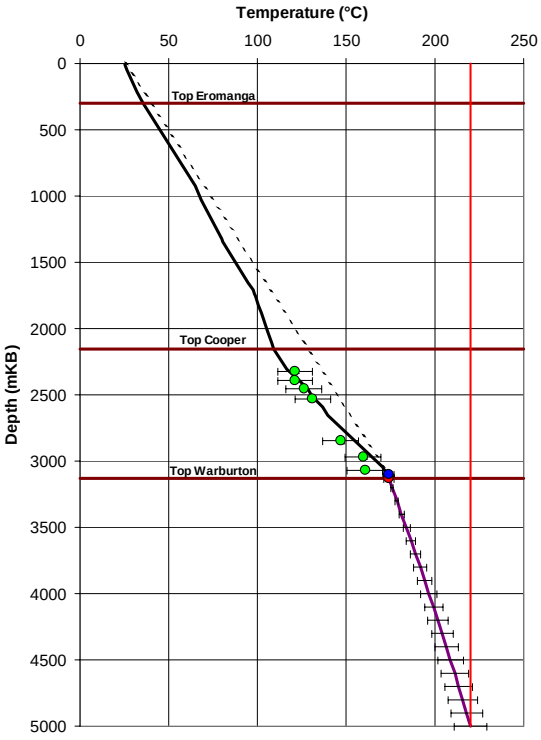

Figure 8. Temperature data and modeled profile for Big Lake 33.

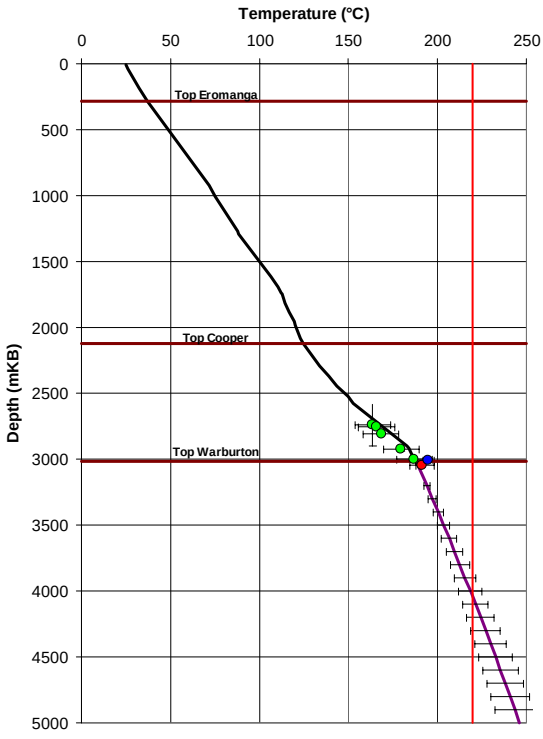

Figure 10. Temperature data and modeled profile for Big Lake 35.

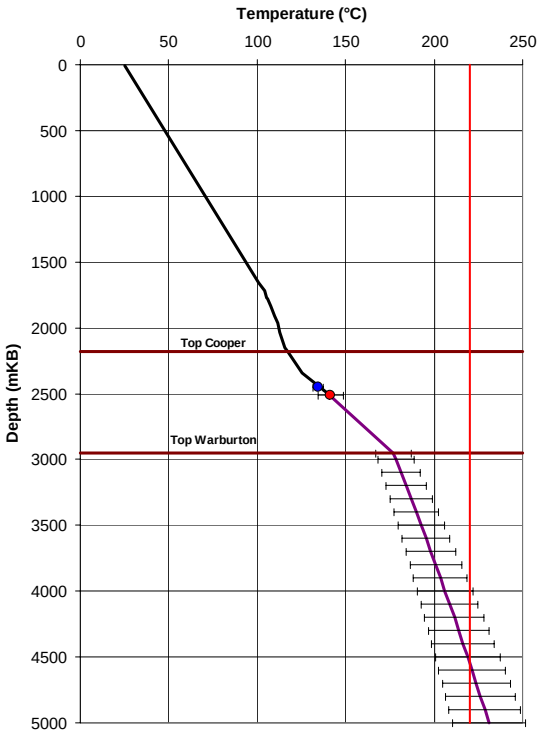

Figure 11. Temperature data and modeled profile for Moomba 15. Note that Top Eromanga horizon was not recorded in PEPS-SA.

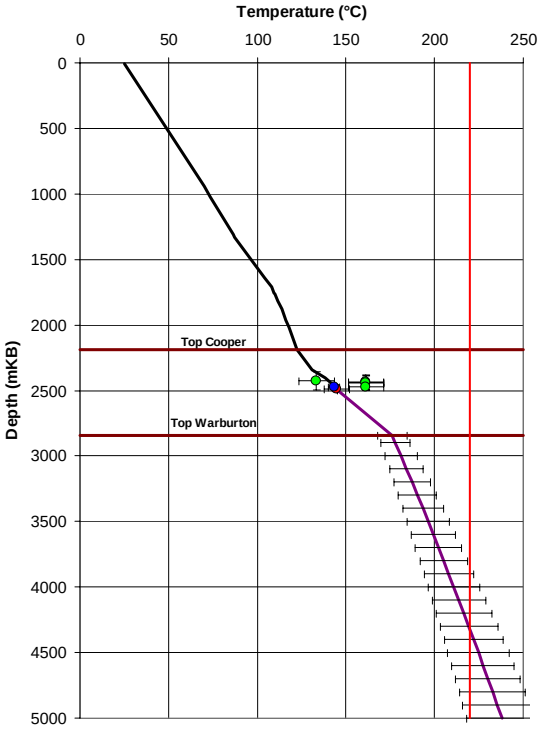

Figure 12. Temperature data and modeled profile for Moomba 17. Note that Top Eromanga horizon was not recorded in PEPS-SA.

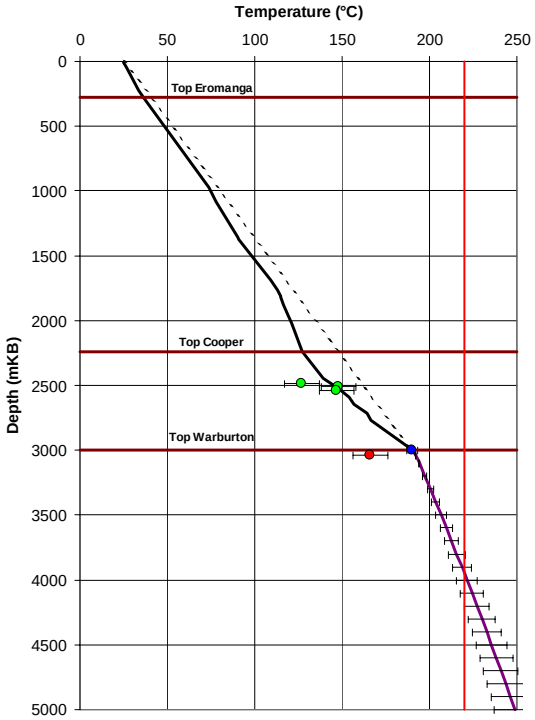

Figure 13. Temperature data and modeled profile for Moomba 50.

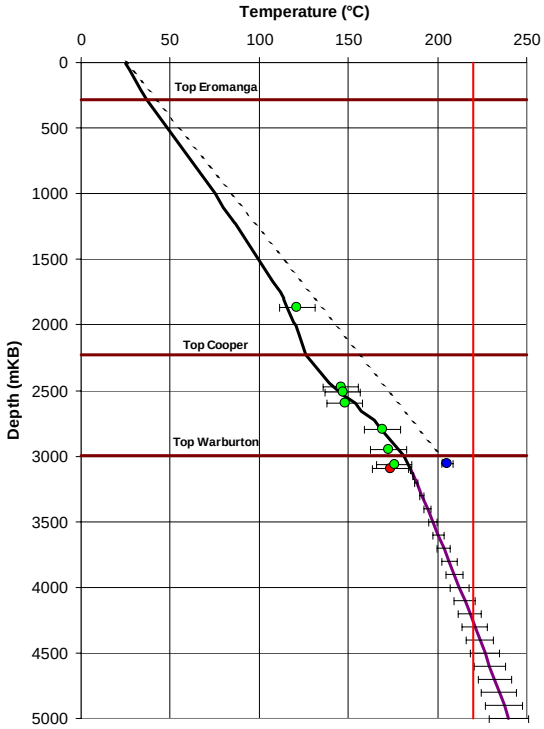

Figure 14. Temperature data and modeled profile for Moomba North 1.

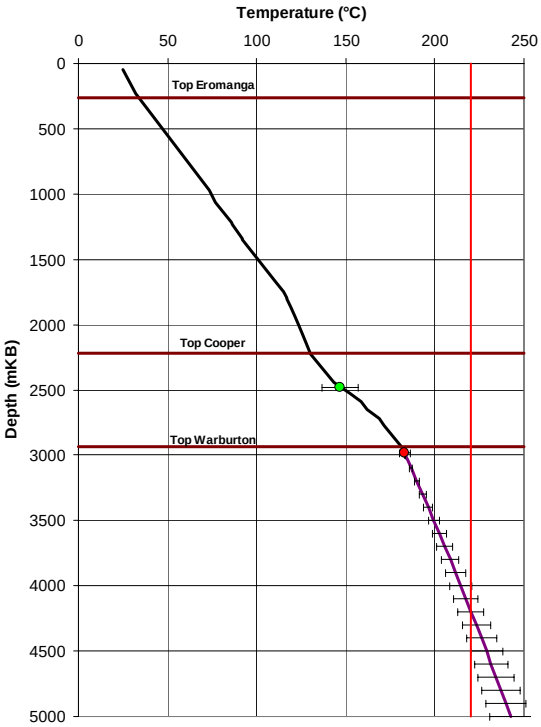

Figure 15. Temperature data and modeled profile for Moomba North 2.

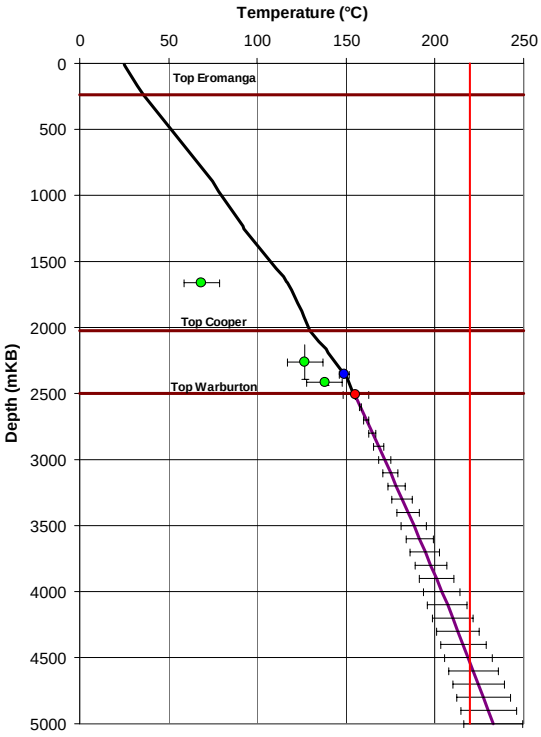

Figure 16. Temperature data and modeled profile for Namur 1.

4. DISCUSSION

In most cases, the modeled temperature profile within each well closely matches many of the reported temperature values. In contrast, straight-line gradients drawn between the surface and CBL values generally do not agree with DST temperatures (Figure 4, Figure 7, Figure 8, Figure 13, Figure 14). This is compelling evidence for the validity of the 1D thermal models, and a basis for strong confidence in the resulting heat flow estimates.

Heat flow estimates are remarkably uniform across the study wells, and at least 50% higher than the global average for Mesozoic aged basins (Jessop, 1990). The magnitude of the estimates is similar to heat flow values previously published for the Cooper Basin (Gallagher, 1987b), although none of the wells from this study were included in the earlier study.

The relationship between heat flow and the Cooper Basin subcrop map (Figure 3) is interesting. The lowest heat flow values (and modeled temperatures) are observed in Big Lake 30 and Big Lake 33. Seismic and well data (Boucher, 2002) suggest that these two wells are located at the edge of, or away from, the granodiorite body. The implication is that there is less heat generated within the crust in those regions where the Big Lake Suite is deeply buried or not present.

If this premise is accepted, then the thermal models may be used to draw conclusions about other wells. For example, Namur 1 may be underlain by a significant thickness of heat-generating granodiorite, although the subcrop map does not suggest this. It may be that Lycosa Formation is only present as a roof pendant above the Big Lake Suite intrusive at that location. The same may be true for the Pando Formation beneath Moomba 17, Big Lake 2, 32, 34 and 35. In contrast, Big Lake Suite may only be present as a thin sill beneath Moomba 15. More wells need to be examined in detail in order to delineate the geographic distribution of heat flow, and its relationship to the Cooper Basin subcrop map.

Because the subcrop map may not accurately delineate the distribution of heat generating basement, all of the models were constructed on the assumption that the wells were underlain by Big Lake Suite granodiorite. If subsequent studies indicate that is not the case for some wells, then the prediction of temperature beneath those wells may be unreliable.

The Moomba North wells were investigated because of a reported temperature value significantly higher than for other wells in the vicinity. PEPS-SA records a CBL temperature of 206°C from a depth of 3053 m in Moomba North 1 (Figure 14). This is well above any temperature from a similar depth in any of the other wells inspected, and suggests that the Moomba North area is very prospective for hot dry rock exploration. However, there are other data from Moomba North 1, including an unreliable Horner corrected bottom-hole temperature (a high degree of scatter on the Horner plot) and a series of seven DST temperatures. None of these are consistent with the high CBL temperature.

Moomba North 2 is located just 2.5 km from Moomba North 1, and penetrated a similar sedimentary sequence. The temperature at 2984 m is 183°C, as suggested by a reliable (very little scatter) Horner plot of three bottom-hole temperatures. This value is strongly supported by the excellent fit of the thermal model to the solitary DST temperature from further up the same well (Figure 15). This result requires a horizontal thermal gradient in excess of 6°C/km if the CBL temperature from Moomba North 1 is

accepted. It is unlikely that such a large horizontal thermal gradient could be sustained between two wells with similar thermal conductivity profiles in close proximity. The simplest explanation is that the CBL temperature from Moomba North 1 is invalid. When that value is ignored, and the Moomba North 1 temperature model is constructed to best fit the DST data, the model very closely matches that of Moomba North 2. Predicted temperatures then vary by only a few degrees Celsius between the two wells at any depth.

5. CONCLUSION

In most cases, temperature data collected from within the Cooper and Eromanga basin sequences beneath permit GEL99 cannot be adequately explained by straight-line temperature gradients. Thermal conductivity contrasts between formations cause significant departures from straight-line gradients. One-dimensional conductive heat flow models, however, accurately predict the observed temperatures in many cases.

The conductive heat flow at the top of the Warburton Basin sequence is about 103±8 mWm^2 beneath most of GEL99. The 220°C isotherm lies at a mean depth of around 4200–4300 m beneath most of the permit. Heat flow may be slightly lower, and the 220°C isotherm slightly deeper, in the vicinity of Moomba 15.

The CBL temperature for Moomba North 1, as recorded in PEPS-SA, appears to be unreliable. When more reliable temperature data are used, heat flow and extrapolated temperatures beneath the Moomba North wells are predicted to be similar to those in other regions of GEL99.

REFERENCES

Beardsmore, G.R. and Cull, J.P.: Crustal heat flow: a guide to measurement and modeling, *Cambridge University Press*, 324pp (2001).

Boucher, R.K.: Report Book 2001/019—Warburton Basin GIS data atlas (CD-ROM). *Department of Primary Industries and Resources, Government of South Australia* (2002).

Deighton, I. and Hill, A.J.: Thermal and burial history. In: Gravestock, D.I., Hibburt, J.E. and Drexel, J.F. (eds.), Petroleum Geology of South Australia Volume 4—Cooper Basin, *Department of Primary Industries and Resources, Government of South Australia*, 143–55 (1998).

Gallagher, K.: Thermal conductivity of sedimentary and basement rocks from the Eromanga and Cooper Basins, South Australia. *Exploration Geophysics*, 18, 381–92 (1987a).

Gallagher, K.: Thermal conductivity and heat flow in the southern Cooper Basin. *Exploration Geophysics*, 18(1/2), 62–7 (1987b).

Jessop, A.M.: Developments in Solid Earth Geophysics Volume 17—Thermal Geophysics. *Elsevier*, Amsterdam, 306pp (1990).

Keen, C.E. and Lewis, T.: Measured radiogenic heat production in sediments from the continental margin of eastern North America: Implications for petroleum generation. *American Association of Petroleum Geologists Bulletin*, 66, 1402–7 (1982).

McKenna, T.E. and Sharp, J.M.: Radiogenic heat production in sedimentary rocks of the Gulf of Mexico Basin, South Texas. *American Association of Petroleum Geologists Bulletin*, 82(3), 484–96 (1998).

Middleton, M.F.: Heat flow in the Moomba, Big Lake and Toolachee gas fields of the Cooper Basin and implications for hydrocarbon maturation. *Exploration Geophysics*, 10, 149–55 (1979).

Sekiguchi, K.: A method for determining terrestrial heat flow in oil basinal areas. *Tectonophysics*, 103, 67–79 (1984).

Swenson, D., Chopra, P. and Wyborn, D.: Initial calculations of performance for an Australian hot dry rock reservoir. *Proceedings World Geothermal Congress 2000, Kyushu-Tohoku, Japan*, 3907–12 (2000).

Touloukian, Y.S., Powell, R.W., Ho, C.Y. and Klemens, P.G.: Thermal properties of matter, Volume 2: Thermal conductivity, non-metallic solids. *IFI/Plenum*, New York and Washington (1970).